

## **Detection of aquifer zones by integration geophysical methods HLEM and VES in the Southeast region of Pará, Brazil**

Herson Oliveira da Rocha<sup>1\*</sup>; João Andrade dos Reis Júnior<sup>2</sup>; Pedro Andrés Chira Oliva<sup>3</sup>; Gildenilson Mendes Duarte<sup>4</sup> & Wagner Ormanes Palheta Castro<sup>5</sup>

<sup>1</sup>Federal Rural University of Amazon (UFRA), Campus de Parauapebas, Rodovia PA-275, Km 7, Zona Rural s/n, 68515-970, Caixa Postal 3017, Parauapebas, PA, Brasil.

<sup>2</sup>Federal Rural University of Amazon (UFRA), Campus de Capanema, Rua João Pessoa 340, Centro, 68700-030, Capanema, PA, Brasil

<sup>3</sup>Federal University of Pará (UFPA), Institute of Coastal Studies (IECOS), Alameda Leandro Ribeiro s/n, Aldeia, 68600-000, Bragança, PA, Brasil

<sup>4</sup>Federal Rural University of Amazon (UFRA), Campus de Tomé-Açu, Rodovia PA-140, 242, 68680-000, Tomé-Açu, PA, Brasil

<sup>5</sup>Federal Rural University of Amazon (UFRA), Cyberspace Institute (ICIBE), Av. Tancredo Neves, 2501, Montese, 66077-530, Belém, PA, Brasil

---

**Abstract:** This work was carried out with the objective of assisting in the construction of a water supply system inside Nova Vida Farm, located in the city of Parauapebas, southeast of the state of Pará, Brazil. The farm is divided into areas for the cultivation of various crops, such as corn, beans, and soybeans, as well as in beef cattle breeding, in confinement, export destination. However, in the dry season, with its insipid supply system, consisting of shallow artesian wells and cisterns for water storage. Based on this, a geophysical study of hydrogeological characterization was carried out, using the measurements of two Vertical Electrical Survey (VES) and 6 electromagnetic profiles with the Slingram system using 8 frequencies (110, 220, 440, 880, 1760, 3520, 7040 and 14080 Hz), where the results are presented in the form of graphs for two VES and in isocontours maps for the profiles by locating and identifying the most promising locations for new wells allocation, which can mean the solution for the management of the supply of water the farm.

**Keywords:** Water Supply; Hydrogeological Characterization; Geophysical Survey

---

Date of Submission: 24-10-2019

Date of Acceptance: 09-11-2019

---

### **I. Introduction**

The lack of water is already a reality in several regions of Brazil and, in addition to the affected population, rural producers already feel their effects on the skin and in the pocket. What used to be a problem unique to the arid regions, today is a constant concern among producers all over the country. In addition to the direct losses in the crop and management caused by lack of water, their scarcity affects the entire productive chain of rural property, directly reflecting production costs (Coelho et al., 2005).

For most producers, the use of water pumps has been a constant need, as well as the search for water solutions such as artesian wells and rainwater catchment tanks. But for this, we must take into account three situations that we can face when we analyze the amount of water available in the possible source of supply: the flow is sufficient in the dry season; Is insufficient in the dry season, but sufficient in average; There is flow, but less than expected consumption. For during a certain period of the year, we will not find enough flow to cover the planned consumption. As on average the flow is enough, then during the rainy season there will be an excess of flow that if properly stored can supply the deficit in the dry season.

The use of irrigation systems is quite common in agriculture and, for many farmers, the support that guarantees the survival of their crops. We can highlight drip irrigation, performed with the use of drilled hoses that distribute water directly into the soil is one of them. The adoption of this type of irrigation represents a reduction of up to 40% in the water consumption and the utilization of the natural capacity of the water distribution soil (Christofidis, 2006; Mantovaniet al., 2007; Pires et al., 2008)

In order to cultivate crops in soils with a large topographic slope, the techniques of fractionation of land lots on steps guarantee a better use of rainwater for irrigation, since it flows with less force and is better used by the soil. Another alternative for water resource economics and optimization is the practice of night irrigation, because it allows better levels of water absorption due to the low amount of evaporation at night (Scaloppi, 2014).

Another alternative for lack of water in rural properties is to invest in reservoirs and rainwater harvesting systems, since the water abstracted can be used in both irrigation and agricultural management processes, as well as in the sanitation of cattle pens. Confinement (Palhares&Guidoni, 2012).

Capturing water directly from the water table is a system widely used by farmers. In addition to the financial economy inherent to this type of solution, because they allocate a large part of the water resources directly to the plantation, the replenishment of the groundwater volume happens in an agile and very efficient way. However, in order for artesian wells to be a viable option, special care must be taken in pumping and transporting water since, according to experts, up to 50% of water resources can be lost only on the way, as well as the allocation of wells to areas productive (Tundisi, 2006).

Obviously, not all water stored underground can be removed under economically viable conditions, especially those located at excessive depths and confined between rock formations. And we defined as objectives of this research, to investigate and map the existence of lithologic and / or subsurface structural discontinuities, locating the most promising areas for groundwater abstraction to drill water wells within a rural property using the methodologies Vertical Electrical Survey (VES) and Slingram in Horizontal Loop Electromagnetic (HLEM) configuration.

## II. Theoretical Aspects

### 21 Electrical Method

The electroresistivity method basically consists of injecting current into the ground, with the intention of measuring the electrical resistivity of the ground through two electrodes called current electrodes (also called electrodes A and B), and measure the potential difference ( $\Delta V$ ) between two other points on the surface, through two more galvanic contacts called potential electrodes (also known as M and N)(Orellana, 1972) (Figure 1).

When we know the inject current  $I$  on the surface and low frequency (less than 10Hz), the potential difference  $\Delta V$  and the value of  $k$  previously tabulated for each of the positions of the electrodes A, B, M and N, we can calculate the Values of apparent resistivity of materials in subsurface through simple algebraic manipulations and trivial laws of physics the apparent resistivity of the layers (Reynolds, 1997). It is known that the electrical resistivity from two current electrodes on the ground surface for a homogeneous and isotropic medium is given Eq. 1:

$$\rho = \frac{1}{2\pi \left( \frac{1}{AM} - \frac{1}{AN} - \frac{1}{BM} + \frac{1}{BN} \right)} \quad (1)$$

where here  $k$  is the geometric function of the arrangement of the electrodes A, B, M and N, named for this geometric factor, given by:

$$k = \frac{\rho \cdot I}{\Delta V} \quad (2)$$

The VES is applied when it is desired to obtain information on the vertical variation of the resistivity where the positions of the current electrodes are regular and symmetrically expanded with respect to the point investigated. The apparent resistivity values are calculated by providing the apparent resistivity curve, which is interpreted quantitatively, directly and intensively, through appropriate software. The models resulting from the surveys can generate geoelectric sections, which can be associated to the section of the geological strata of the subsurface.

### 22 Electromagnetic Method

The electromagnetic methods can be classified in two ways. In the first, we say that they act in the Time Domain (TEM), where the excitation is by pulse of current in the transmitting coil followed by reception of the transient and, in the second, in the Domain of Frequency (FEM), where the instruments use one or more frequencies for data collection in which transmitter and receiver operate tuned and together. The electromagnetic methods are based on the principle of electromagnetic induction, which, in turn, record the response from an interaction between the electromagnetic wave and the subsurface.

In the process of electromagnetic induction, an electric current that varies with time, circulates in a transmitting coil (Tx). For this reason, the current generates an oscillating magnetic field-primary field- ( $H_p$ ) of the same frequency and phase. Lines of primary magnetic field forces penetrate the subsurface and consequently the conducting body. When this happens an electromotive force (or voltage) appears on the conductor. Thus, a current will flow within the conducting body in response to the induced electromotive force.

This current normally flows in the conductor in planes perpendicular to the lines of force of the transmitted primary magnetic field. The current flowing inside the conductor generates another field, called the secondary magnetic field ( $H_s$ ), whose lines of forces are opposed to the variation of the primary magnetic field and thus a complete response to this induced current is obtained by the fact that there is a combination of the

primary and secondary magnetic field. The resultant of this combination of  $H_p$  and  $H_s$  is measured by the induction of a receiver coil (Rx) (Figure 2).

The use of two coils in the electromagnetic method characterizes what is called the Slingram system. In this system, the two coils can be arranged according to several orientations, for example: (a) arrangement of both coils in a horizontal plane, constituting the horizontal coplanar arrangement, vertical dipole or HLEM; (b) arrangement of both coils in the same vertical plane, constituting the vertical coplanar arrangement or horizontal dipole and (c) arrangement in which the transmitting coil is placed in the vertical plane and the receiving coil is placed in the horizontal plane, constituting the vertical loop arrangement (Pinéo, 2005; Medeiros, 2008).

The Slingram system operates within a range of low induction numbers, known as Low Induction Numbers (LIN) where the product ( $\omega\sigma s^2$ ) is less than 1000, described by the equation below (McNeill, 1980; Thielsson et al., 2011):

$$\frac{H_p}{H_s} = \frac{i\omega\mu_o\sigma^2 H_p}{4 H_s} = \frac{i\omega\mu_o\sigma s^2}{4} \quad (3)$$

Where  $H_p$  is the primary magnetic field;  $H_s$  is the secondary magnetic field;  $\omega$  is the angular frequency ( $\omega=2\pi f$ ),  $f$  is the frequency (Hz);  $\mu_o$  is the magnetic permeability of space;  $\sigma$  is the electrical conductivity of the subsurface (mS/m);  $s$  is the distance between the coils (give in meters) and is the complex number. After calculating the rate between the secondary and primary field ( $H_p/H_s$ ) and from Eq. (3), we found the apparent conductivity ( $\sigma_a$ ) which is indicated by the instrument by the equation below:

$$\sigma_a = \left(\frac{4}{i\omega\mu_o\sigma s^2}\right) \cdot \left(\frac{H_p}{H_s}\right) \quad (4)$$

In addition, we have two models of dipoles: Horizontal Dipole (HD), where the coil axes are positioned vertical and the depth of investigation is about 0,75 times the spacing of the coil and the Vertical Dipole mode (VD), that is, with the coil axes arranged horizontal and the depth of investigation is about 1,5 times the spacing of the coils (Dondurur, 2005).

### III. Study Area

The city of Parauapebas is in Southeast region of the State of Pará and distance 547 km from de capital Belém. The central area has the following geographic coordinates: 06° 03' 3'' South latitude and 49° 55' 15'' longitude Wst of Greenwich. I border on the North with the city of Marabá, on the East with the city Curionópolis, on the South with the cities of Canaã dos Carajás and Água Azul of North, and, at the end, on the West with São Félix do Xingu (PMP, 2009).

To get to the headquarters of the Nova Vida Farm, where the measures were carried out, we left Marabá on State highway PA-150, as far as Eldorado of Carajás distant about 100 km. Continuing trip now by State highway PA-275 to the center of the city of Parauapebas distant about 66 km. From there we continue along another Satate highway PA-275 to the entrance gate of the Nova Vida Farm, distant about 25 km from Parauapebas (Figure 3).

The city presents a topography with great variation of is altimetric levels, where the highest values verified in the mountains of the Carajás, Arqueada, Buriti and Rabo, oscillating between 800 and 900 meters and the lower levels between 200 and 210 meters. Geographically it is marked by an area with a rugged landscape where the mountains predominate. It has the main elevations that the Carajás, a set of mountains where are de mineral reserves.

It present a complex geological structure, defined by a variation of Precambrian rocks, inserted inside the Xingu Complex (granites, granodiorites, diorites, migmatites, basic granules and acids, shale, quartzite e gneisses); Grão-Pará Group, covering the mineral province of Carajás (jaspilites, hematites, metabasites, ferruginous quartzites, metabasites, quartzites, itabirite and phyllites); sediments of the River Fresco Formation and Membro Azul (manganese shales, carbonaceous, silty, argillite, grauvacas and conglomerate sandstones); Granite Serra dos Carajás (granite profiritic of alaskitic tendency, with feldpathic and pematiform apophyses) and, finally, granite rocks Old Guilherme (granites e granodiorites), subvolcanic and intrusive (DOCEGEO, 1988; Dall'Agnol et al., 1994; Costa et al., 1995; Pinheiro e Holdsworth; Leite et al., 2004; Ferreira et al., 2008; Feioet et al., 2012).

The main hydrographical basin is that of the rives Itacaiunas, which rises Southwest of the territory, in Serra of Seringa, and crosses mountains area that include the Serra dosCarajás, bordering in part with the Marabá city. Its tributaries are: by the right bank, the Novo River (limit with the city Curionópolis) and Parauapebas, that bathes the municipal seat. On the left bank, the Rivers Água Preta, Piranhas and Caeté (Siqueira et al., 2012).

#### IV. Material and Methods

##### 41 Vertical Electrical Survey (VES)

The data of the with the electroresistivity method consisted of measures of apparent resistivity, taken through the application of VES in the Schlumberger arrangement. Two VES were executed inside Nova Vida Farm and the equipment used in the measurements was the Resistivimeter X5 manufactured by company AutoEnergia Inc.

The surveys were made with minimum distance between the electrodes of current equal to 2 meters ( $AB/2=1$  meter) and the maximum equal to 200 meters ( $AB/2=100$  meters). The maximum distance between the electrodes was imposed by the conditions of the terrain, avoiding strong topographic differences, observing conditions of access for the expansion of the electrodes a limitation of the equipment. Because with these openings of the current electrodes, one can get a response from depths within the objectives of this research.

##### 42 Slingram (HELM)

In all, 6 profiles with electromagnetic measurements with the equipment Slingram MAX MIN I, manufactured by the company APEX Parametrics, were executed according to the HLEM arrangement, with  $T_x-R_x= 50$  m, taking the amplitude of the components in-phase (real part) and in quadrature (imaginary part) of the Secondary Field (Hs) in the eight frequencies (110, 220, 440, 880, 1760, 3520, 7040, 14080 Hz) available in the system. The use of the eight frequencies allows the investigation in vertical and combined with the horizontal profiling (lateral investigation) we obtain an image of the subsurface below the profiles. Are, therefore, 16 parameters measured in each station that allow a good depth scan.

#### V. Results and Discussions

##### 51 VES

For the interpretation of VES data, the Interpex IX1 Dv2 inversion software was used, which allows to calculate the apparent resistivity for a certain theoretical model of horizontal, homogeneous and isotropic layers (Interpex, 1993). The apparent resistivity values measured in the VES were plotted in bilogarithmic graphs and then smoothed to eliminate the geological noise intruded in the measurements, usually due to lateral variations in the geological layers. In some case, unreliable values (values that are very different from adjacent values) have been replaced by others obtained from interpolation or extrapolation of reliable values.

In VES 1 it is possible to interpret a 6 layer model, and the two most superficial layers present resistivity values varying 1056  $\Omega.m$  and 2043  $\Omega.m$  respectively, represented by sandy sediments, typical or red-yellow latosol for first layer, with is a depth of approximately 1.1 m and a red-yellow argisol and a thickness of 2.3 m; in the third layer at 3.4 m depth, the resistivity decreases to 21  $\Omega.m$  which shows the infiltration and accumulation of water in this infiltration and accumulation of water in this layer forming a film between zones. Below, at 7 m, a very resistive extract (3900  $\Omega.m.$ ) occurs that can be related to granites of the River Fresco Formation. And below this succession of layers an extract with resistivity varying from 41 to 50  $\Omega.m$ , interpreted as a zone of capillarity highly promising to the exploration of underground water (Figure 4).

The VES 2 also obtained a response corresponding to a 6-layer model, which according to the model generated from the collected data we have the first two highly resistive layers (1004 and 1484  $\Omega.m$ ), similar to what was presented in VES 1. Below we have a third layer with 23 m of thickness and resistivity around 263  $\Omega.m$  whose test shows a model of sand-clayer layer that can be represented by the presence of a perennial aquifer. Afterwards, we observed a resistive layer (1669  $\Omega.m$ ) and the depths below can be observed as successions of layers propitious to the saturated zone (42 to 46  $\Omega.m$ ) with thicknesses of 13.7 m and 9.8 m respectively (Figure 5).

The Table 1 shows the parameters obtained for each survey where we can verify the number of layers of the model, the resistivity of each layer (R), give in  $\Omega.m$  and the thickness (H) in meters.

**Table 1** Layer model parameters

	SEV_01		SEV_02	
	Resistivity ( $\Omega.m$ )	Thickness (m)	Resistivity ( $\Omega.m$ )	Thickness (m)
1	1056.0	1.1455	1004.6	1.3
2	2043.4	2.2692	1484.5	3.4
3	21.365	2.4797	263.9	23
4	3994.1	7.0182	1669.2	23.6
5	41.834	17.018	42.5	37
6	50.415	17.804	46.5	47.2

Based on the parameters of Table 1, we constructed a potentiometric map of the aquifer zone along with the vector map indicating the normal Direction of the groundwater flow (Figure 6). Based on the map of figure 4 we observed 3 zones; the first on the SO direction where we observe an upper layer, with resistivities varying between 900 and 1050  $\Omega$ .m, with a thickness of 0.9 and 1.5 meters, predominantly sandy, that must correspond to the sediment pack of the cover.

A central zone can also be observed in the map where it presents a very conductive layer with resistivities of 21 to 265  $\Omega$ .m with thicknesses of 2 to 23 meters, presenting a narrowing and arching around the VES 1, being able to be related to a clay layer where probably should be the local water aquifer environment. It is worth remembering that this zone may also be related to the infiltration of water stored in an underground cisterna located in front of the grain storage shed.

Finally, a third region, located in the NW Direction below the second and third layers, showed a layer with a resistivity between 40 and 1.600  $\Omega$ .m and a thickness between 17 and 23 meters, which should contain a rocky layer and the values of be a confined aquifer or the accumulation of water in rock fractures.

Figure 6 shows the contour map obtained from VES 1 and 2. It is possible to identify two regions, the first one located to the southwest, a region of lower depth and resistivity around 1300  $\Omega$ .m (brown), where the top of the sediment are closer to the surface. And another to the northeast (blue), presenting less resistive characteristics (below 150  $\Omega$ .m), being more conducive to the location of more promising zones for well allocation.

## **52 Slingram**

The data obtained with the MAX MIN I system are presented in contour map format of the in-phase component of the secondary field ( $H_s$ ) for each of the eight analyzed frequencies. For the depth investigations, i.e., at the frequencies of 110 Hz, 220 Hz, 440 Hz e 880 Hz (Figures 7, 8, 9 and 10) and for shallower investigations at frequencies 1760 Hz, 3520 Hz, 7040 Hz e 14080 Hz (Figures 11, 12, 13 and 14) and block diagram 3D for all the profiles run in Nova Vida Farm.

Based on the characteristic response of the HLEM, where the in-phase component exhibits negative peak anomaly on the conductive body, the maps and 3D diagram block were constructed from varied red and yellow color spectrum representing resistive portions to blue representing the portions conductivity of the subsurface in which the values range from -5 to 100 (Figures 7, 8, 9, 10, 11, 12, 13 and 14).

The other form of visualization of this multi-frequency electromagnetics sweep is made in the 3D diagram block (Figure 15). In it can find the most promising zones for collecting underground water in depth aquifers and in shallower free aquifers because in the block diagram, we have a tree-dimensional visualization of the problem in question.

The maps corresponding to the frequencies 14080, 7040, 3520 e 1760 Hz (Figures 14, 13, 12 and 11) show the electromagnetic response of the shallower distribution of the layers and are well correlated with the responses of the two VES. From the frequency 880 Hz, the maps show almost no values corresponding to conductive zones, indicating resistive bodies in depth up to the frequency of 110 Hz (Figures 10, 9, 8 and 7).

## **VI. Conclusions**

Since the joint interpretation of the geophysical data, a standard of characterization of the shallow subsurface has been established, providing information on the geological layers and hydrogeological parameter in Nova Vida Farm, and the results of the geophysical methodologies (VES and Slingram) presented an excellent correlation between each other ensuring the reduction of ambiguities.

The interpretation of the surveys revealed three distinct zones; a shallower, corresponding to a lower resistivity substrate, ranging 41 to 50  $\Omega$ .m and, between these two zones, a transition zone that is related to the interface of the River Fresco Formation. Based on the interpretation of the electromagnetic response, it was possible to identify and delimit the most promising zones for water prospection and to inter that the free aquifer located between layers 3 and 4 loses its recharge power precisely during the dry season, therefore the necessity to explore depth water to allocate wells. And, for this, we can have observed the answers obtained with the MAX MIN I for the four lower frequencies where the maps and 3D block indicate conductive zones in depth.

Thus, we suggest two holes and they are designed to remove water from the fourth and sixth layers. This is because, by the surveys, below the fourth layer, the substrate is conductive and should correspond to a packet of shale or water accumulation in rock fractures as well as a confined aquifer. The figure 15 providing the most suitable and being the most promising for new catchment areas and for drilling holes to construct new supply wells. We indicate two locations for allocation of two well (P1 and P2); the first shallower (blue color) and the second, depth (red color) to meet the demands of the Farm.

## References

- [1]. Coelho, E. F.; Coelho Filho, M. A.; & Oliveira, S. D. 2005. Irrigated agriculture: water use irrigation efficiency. *Bahia Agrícola*, 7 (1): 57-60 (in Portuguese)
- [2]. Costa J. B. S.; Araújo O. J. B.; Santos A., João, X. S. J.; Macambira, M. J. B.; Lafon, J. M. A. 1995. Mineral Province: Tectono-Structural, Stratigraphic and Geochronological Aspects. *Boletim do Museu Paraense Emílio Goeldi. Série Ciência da Terra*(7): 199-235 (in Portuguese)
- [3]. Christofidis, D. 2002. Cerrado water resources and their potential for irrigation use. *Jornal Item*, 60 (1): 87-97 (in Portuguese)
- [4]. Dall'Agnol, R.; Lafon, J.M. & Macambira, M.J.B. 1994. Proterozoic anorogenic magmatism in the Central Amazonian Province: geochronological, petrological and geochemical aspects. *Mineralogy and Petrology* (50): 113-138. <https://doi.org/10.1007/BF01160143>.
- [5]. Docegeo. 1988. In: 25<sup>th</sup> SBG Brazilian Geology Congress. Expanded Summaries, São Paulo, p. 11-56 (In Portuguese).
- [6]. Dondurur, D. 2005. Depth Estimates for Slingram Electromagnetic Anomalies from Dipping Sheet-like Bodies by the Normalized Full Gradient Method. *Pure and Applied Geophysics*. (162): 2179-2195. <https://doi.org/10.1007/s00024-005-2711-x>.
- [7]. Feio, G. R. L.; Dall'Agnol, R.; Dantas, E. L.; Macambira, M. J. B.; Gomes, A. C. B.; Sardinha, A. S.; Oliveira, D. C.; Santos, R. D.; Santos, P. A. 2012. Geochemistry, geochronology, and origin of the Neoproterozoic Planalto Granite suite, Carajás, Amazonian craton: A-type or hydrated charnockitic granites? *Lithos*. (151): 57-73. <https://doi.org/10.1016/j.lithos.2012.02.020>.
- [8]. Ferreira, A.T.R.; Almeida, J. A. C.; Dall'Agnol, R. 2008. Geology and Magnetic Petrology of the Bannach Dikes, Rio Maria Granite-Greenstone Terrain, Southeast Pará. In: IVSBG Volcanism Symposium and Associated Environments, Foz do Iguaçu (in Portuguese).
- [9]. Interpex Limited. 1993. RESIX IP v. 2.0 - DC Resistivity and Induced Polarization Data Interpretation Software. User's Manual. INTERPEX Limited, Golden, Colorado, U.S.A., 299 p.
- [10]. Leite, A. A. D. S.; Dall'agnol, R.; Macambira, M. J. B.; & Althoff, F. J. 2016. Geology and geochronology of Archean granitoids from Xinguara-PA region and its implications on the evolution of Rio Maria granite-greenstone terrain, Amazonian Craton. *Brazilian Journal of Geosciences*, 34 (4): 447-458. (in Portuguese)
- [11]. Mantovani, E. C.; Mantovani, E. C.; Bernardo, S., & Palaretti, L. F. 2006. Irrigation: Principles and Methods. Viçosa, Editora UFV, 380 p. (in Portuguese)
- [12]. Medeiros, A. R. C. 2008. Geophysical and hydrogeochemical measurements applied to groundwater exploration in a saltwater intrusion environment in the village of Algodão-PA. Graduation Thesis. Federal University of Pará. 87p. (in Portuguese)
- [13]. Pinó, T. R. G. 2005. Integration of geophysical, geological and sensory data applied to groundwater exploration in fissural environment (Juá District, Irauçuba / CE). Master's Thesis. Federal University of Ceará. 122p. (in Portuguese)
- [14]. Orellana, E. 1972. *Prospección Geoelectrica en Corriente Continua*. Madrid, Editora Paraninfo, 523p.
- [15]. Palhares, J. C. P. & Guidoni, A. L. 2012. Quality of rainwater stored in cisterns used for desedimentation of swine and beef cattle. *Ambi-Água*, (7): 244-254. <http://dx.doi.org/10.4136/ambi-agua.822>. (in Portuguese)
- [16]. Pinheiro, R. V. L. & Holdsworth, R. E. 1997. The Structure of the Carajás N-4 Mine Ironstone deposit and associated rocks: Relationship to Archean strike-slip tectonics and basement reactivation in the Amazon region, Brazil. *Journal of South American Earth Sciences*. (10): 305-319. [https://doi.org/10.1016/S0895-9811\(97\)00018-7](https://doi.org/10.1016/S0895-9811(97)00018-7).
- [17]. Pires, R. C. M.; Arruda, F. B.; Sakai, E.; Calheiros, R. O.; Brunini, O. 2008. Irrigated Agriculture. *Journal of Agricultural Technology and Innovation*, (1): 98-11. (in Portuguese)
- [18]. P.M.P. 2009. Information, tourism and entertainment. Computer Coordination. Social Media Advisory. Available at <http://www.parauepebas.pa.gov.br>. Access on 25 jun. 2018. (in Portuguese)
- [19]. Reis Jr, J. A.; Castro, D. L.; Jesus, T. E. S.; Lima Filho, F. P. 2014. Characterization of collapsed paleocave systems using GPR attributes. *Journal of Applied Geophysics*, (103): 43-56. <https://doi.org/10.1016/j.jappgeo.2014.01.007>.
- [20]. Reynolds, J. M. 1997. *An Introduction to Applied and Environmental Geophysics*. John Wiley & Sons, 2<sup>nd</sup> Edition, 712p.
- [21]. Scaloppi, E. J. 2014. *Low cost irrigation in rotational grazing systems*. São Paulo, Academic Culture Publisher, 105p. (in Portuguese)
- [22]. Siqueira, G.W.; Aprile, F.; Miguéis, A. M. 2012. Siqueira, G. W., Aprile, F., & Miguéis, A. M. 2012. Water quality diagnosis of Parauapebas river (Pará - Brasil). *Acta Amazonica*, 42 (3): 413-422. <https://doi.org/10.1590/s0044-59672012000300014>
- [23]. Thielsson, J.; Rousselle, G.; Simon, F. X.; Tabbagh, A. 2011. Slingram EMI prospection: Are vertical orientated devices a suitable solution in archaeological and pedological prospection? *Journal of Applied Geophysics*. (75): 731-737. <https://doi.org/10.1016/j.jappgeo.2011.10.002>.
- [24]. Tundisi, J. G. 2008. *Recursos hídricos no futuro: problemas e soluções*. Estudos Avançados, 22(63): 7-16. <http://dx.doi.org/10.1590/s0103-40142008000200002>

## Figure Captions

Figure 1: Schematic model of the Schlumberger arrangement in SEV's in field operation (Oliva et al, 2010)

Figure 2: Principle of operation of the electromagnetic induction tools

Figure 3: Study area and location of the Parauapebas city

Figure 4: Graphic Contains VES 1

Figure 5: Graphic Contains VES 2

Figure 6: Isopach of maps the layers

Figure 7: Map of the phase component for frequency of 110Hz

Figure 8: Map of the phase component for frequency of 220Hz

Figure 9: Map of the phase component for frequency of 440Hz

Figure 10: Map of the phase component for frequency of 880Hz

Figure 11: Map of the phase component for frequency of 1760Hz

Figure 12: Map of the phase component for frequency of 3520Hz

Figure 13: Map of the phase component for frequency of 7040Hz

Figure 14: Map of the phase component for frequency of 14080Hz

Figure 15: Block 3D diagram of the in-phase component for the 8 frequencies indicating the best locations for well allocation

Figure 1

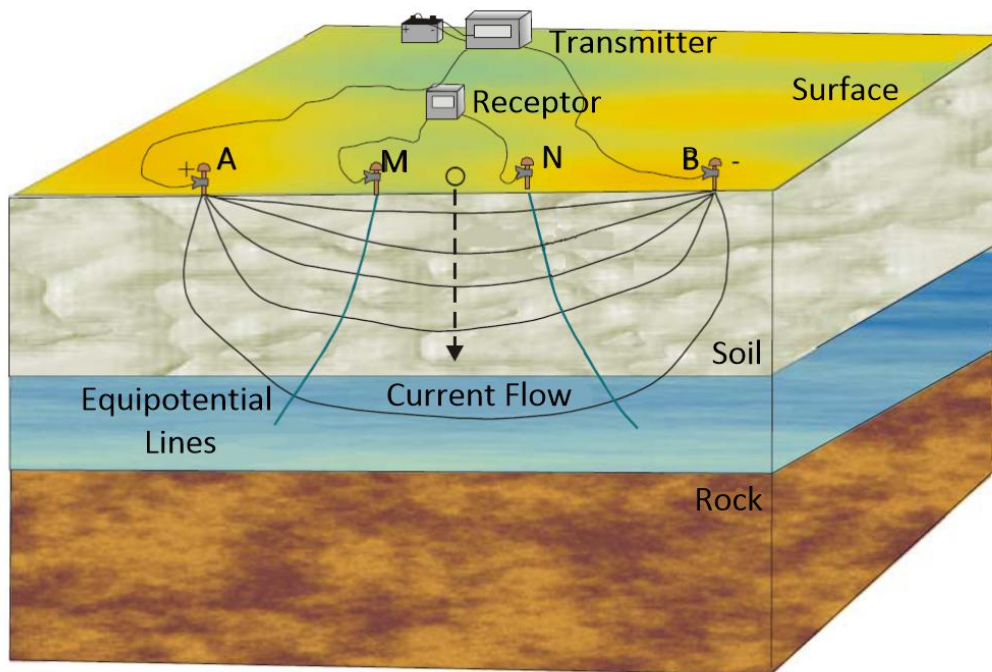


Figure 2

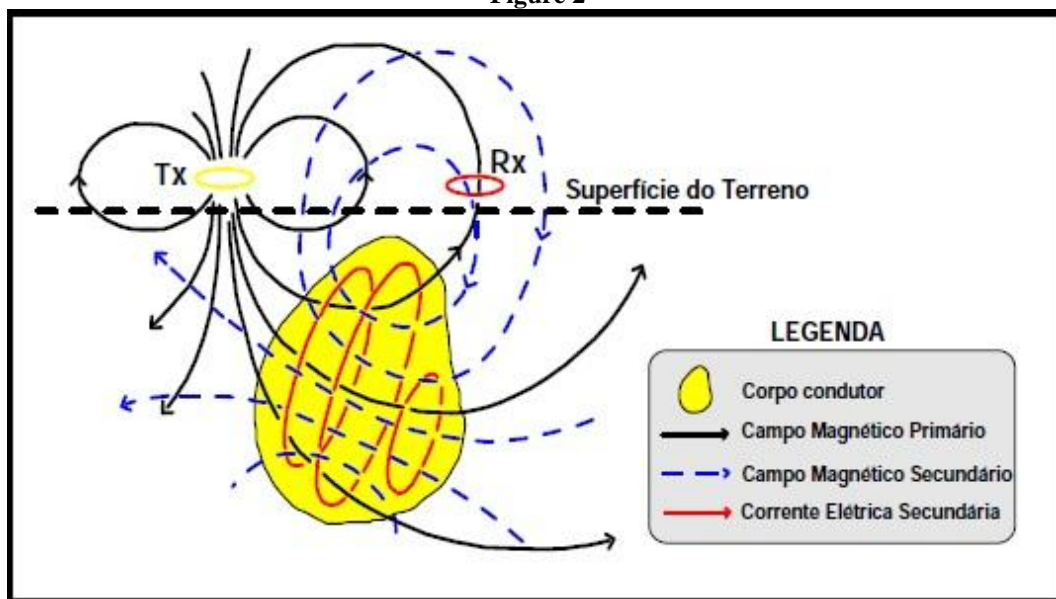


Figure 3

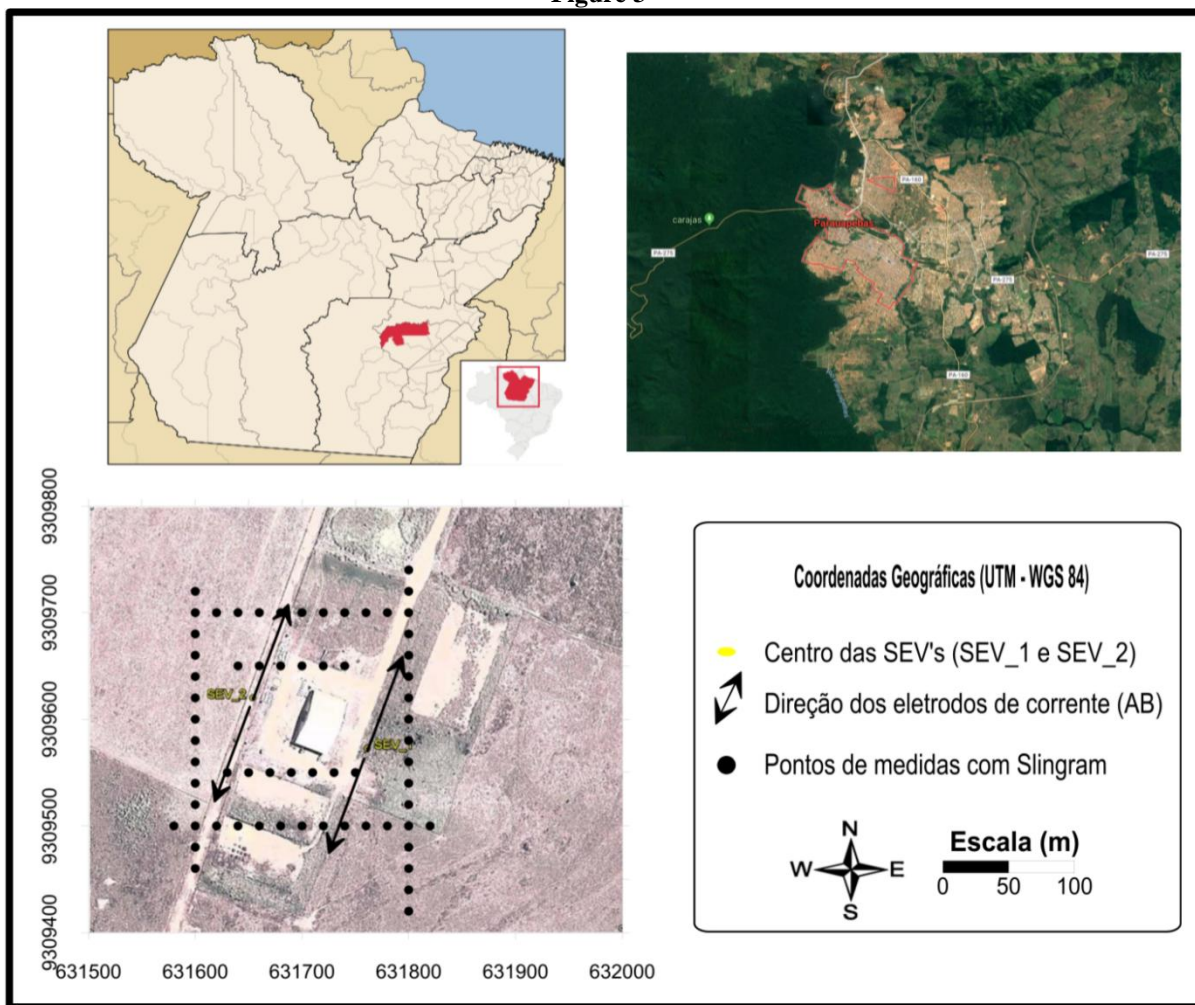


Figure 4

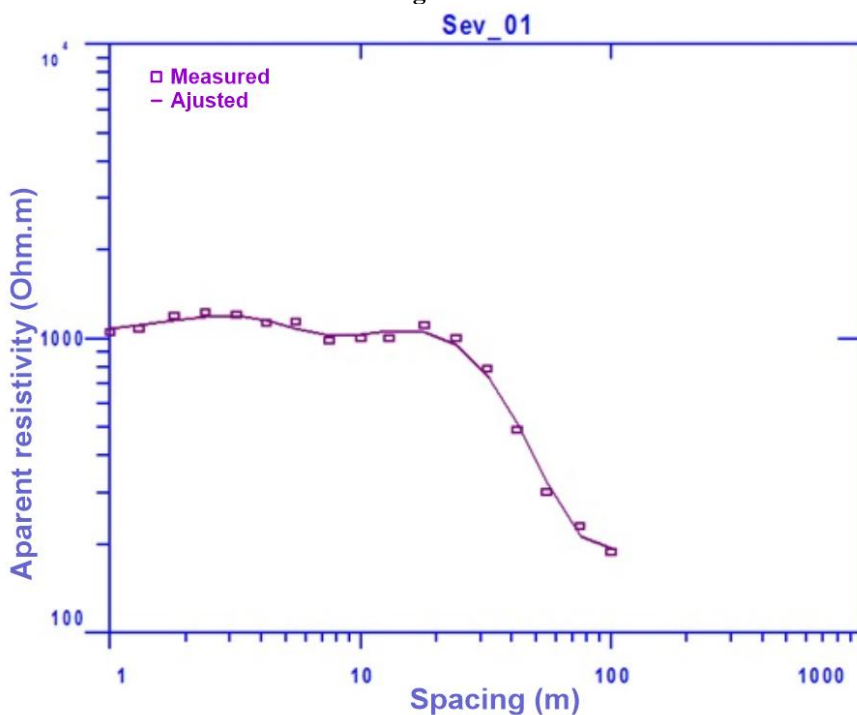




Figure 5

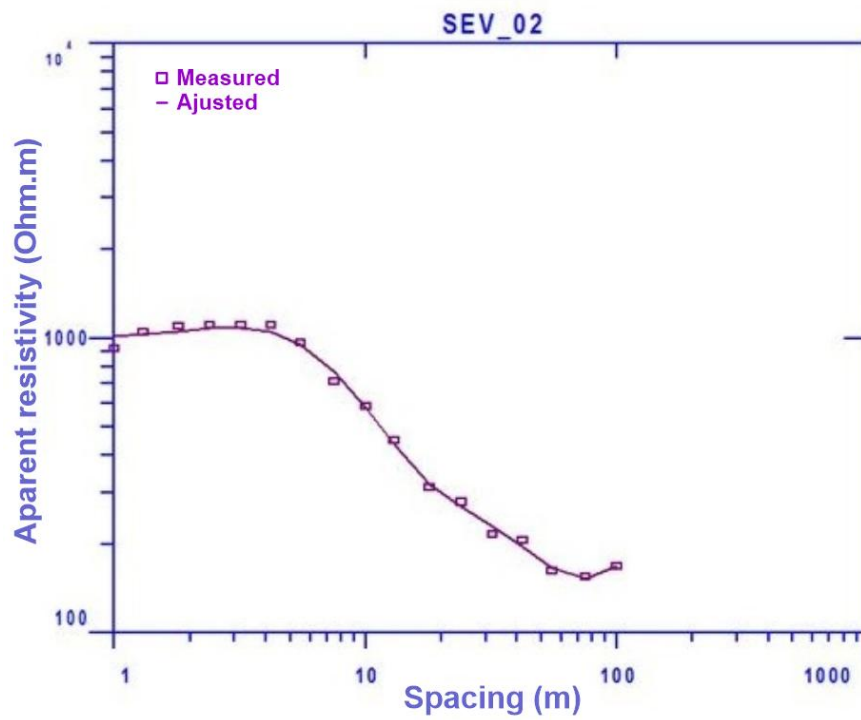


Figure 6

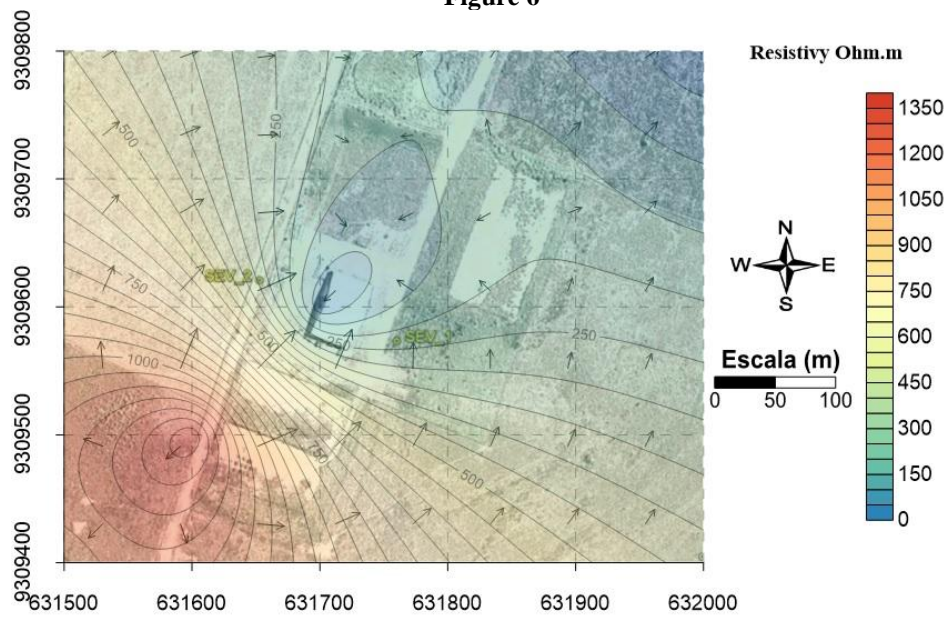


Figure 7

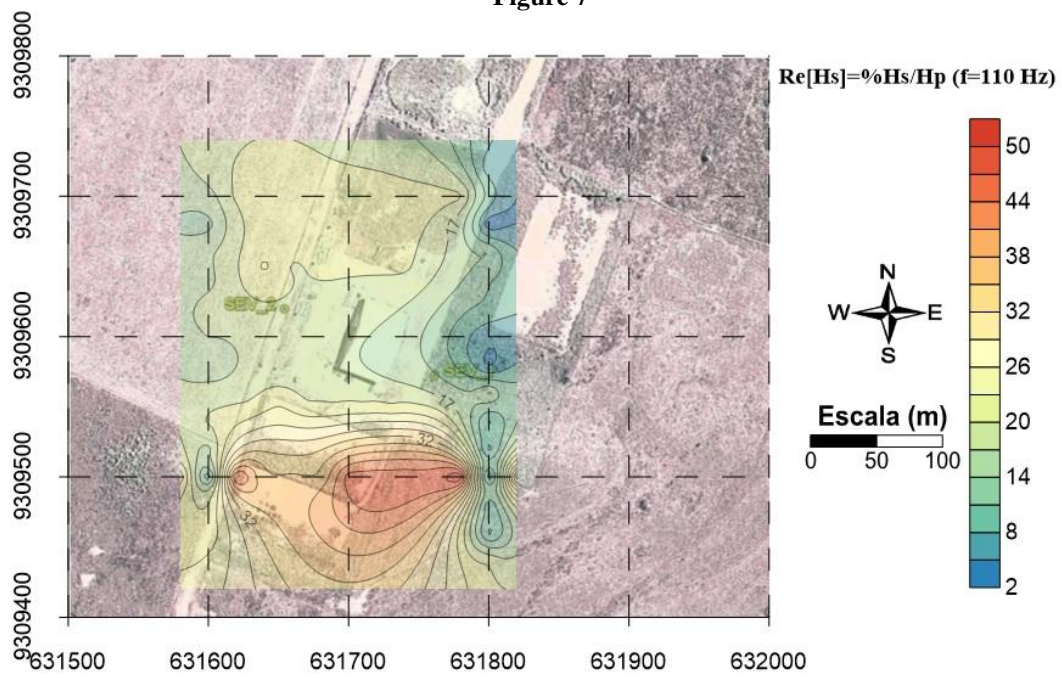


Figure 8

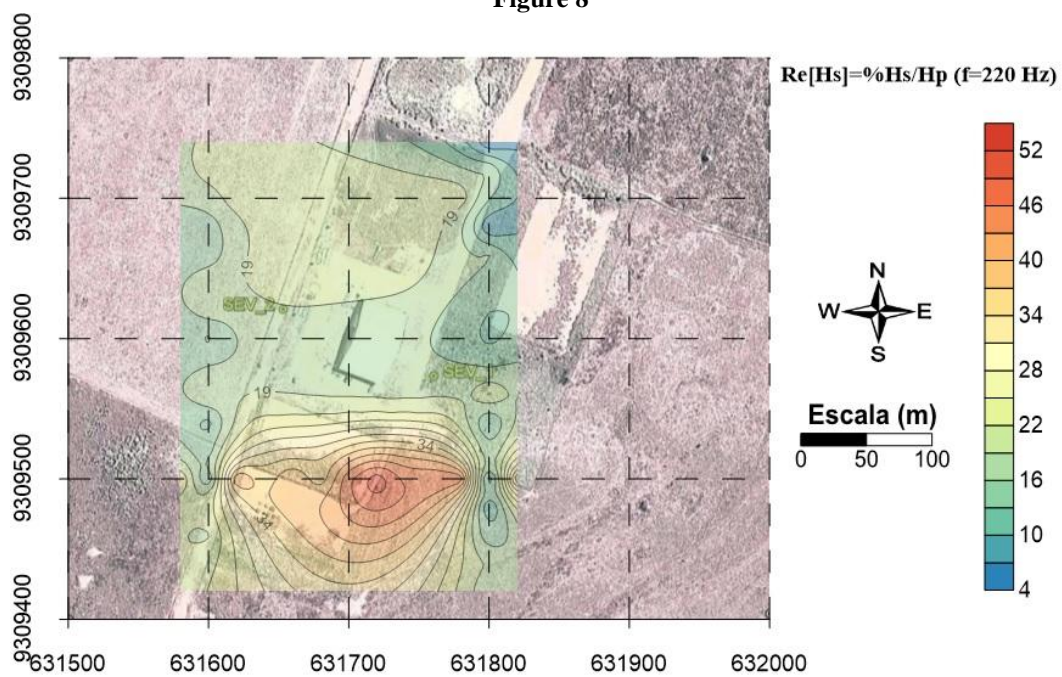


Figure 9

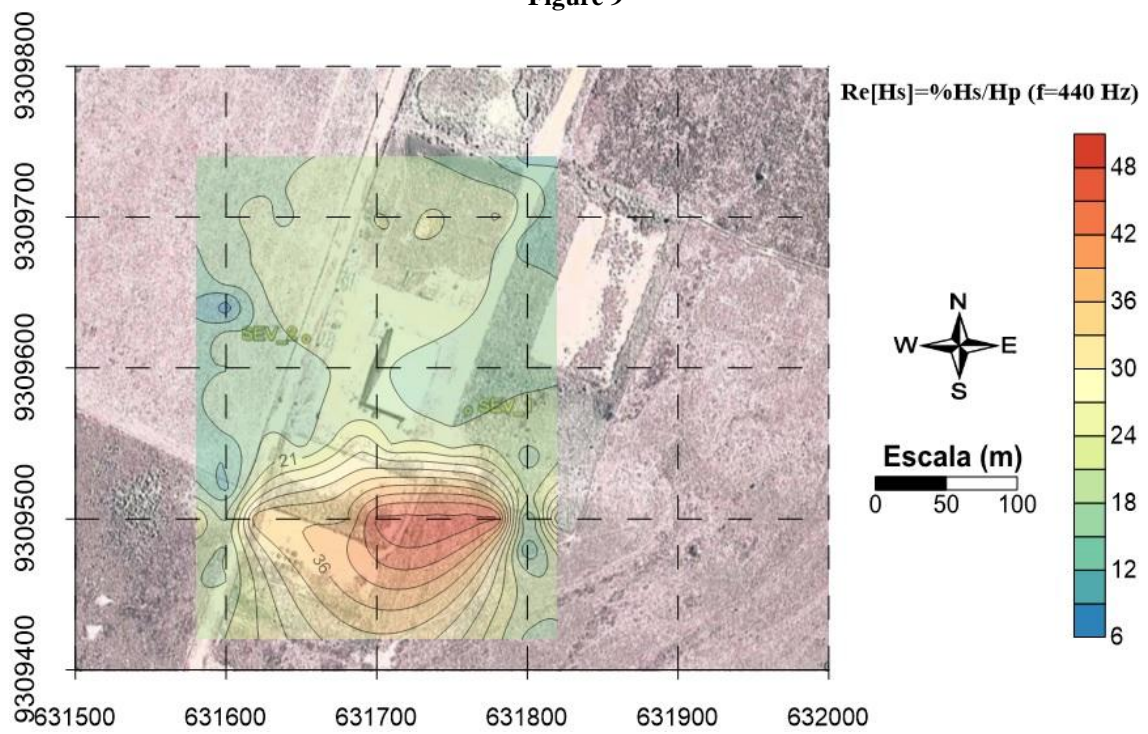


Figure 10

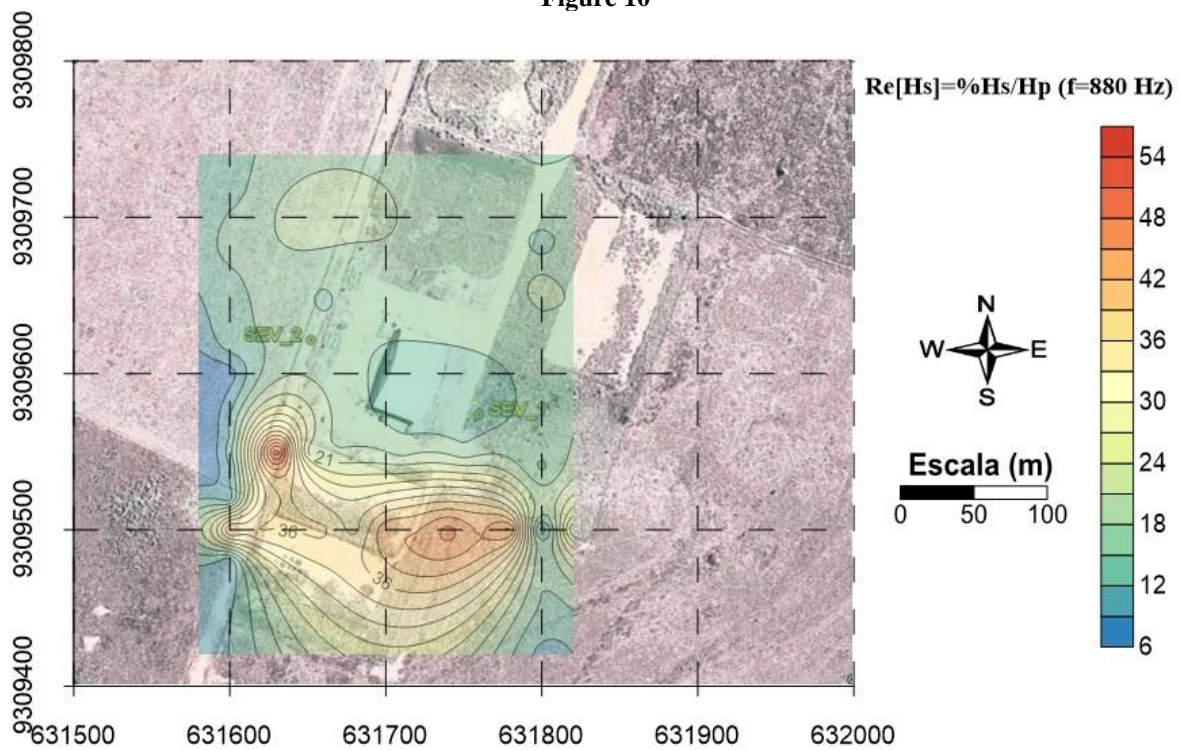


Figure 11

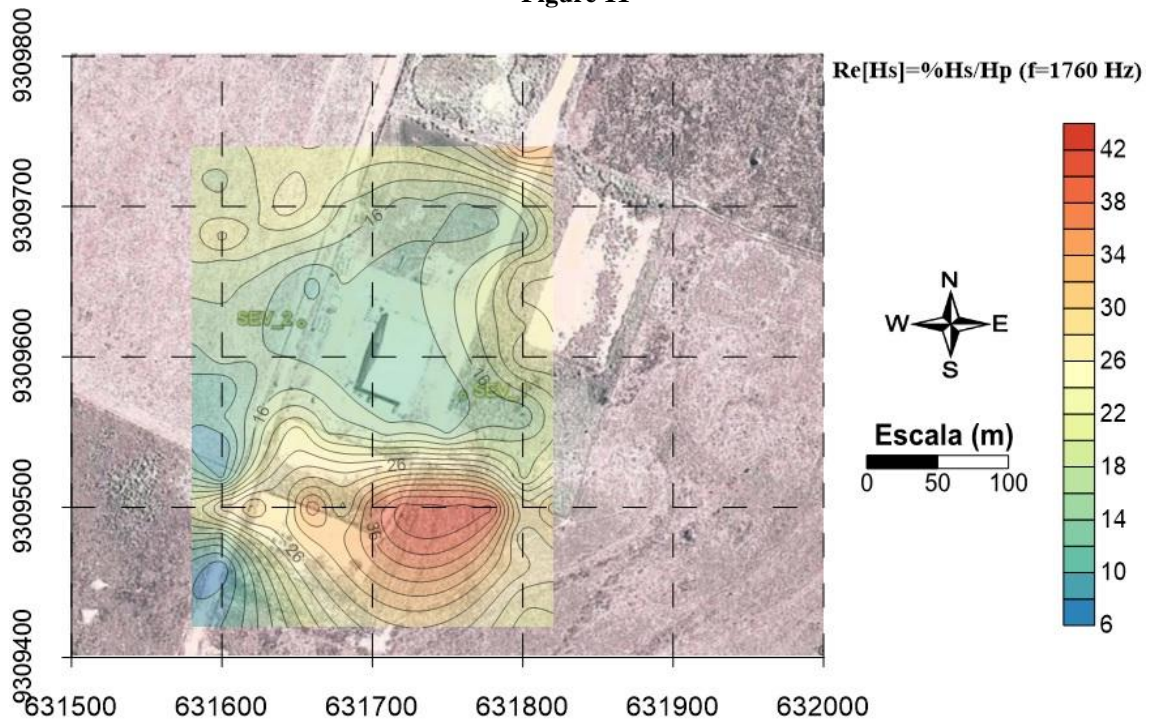


Figure 12

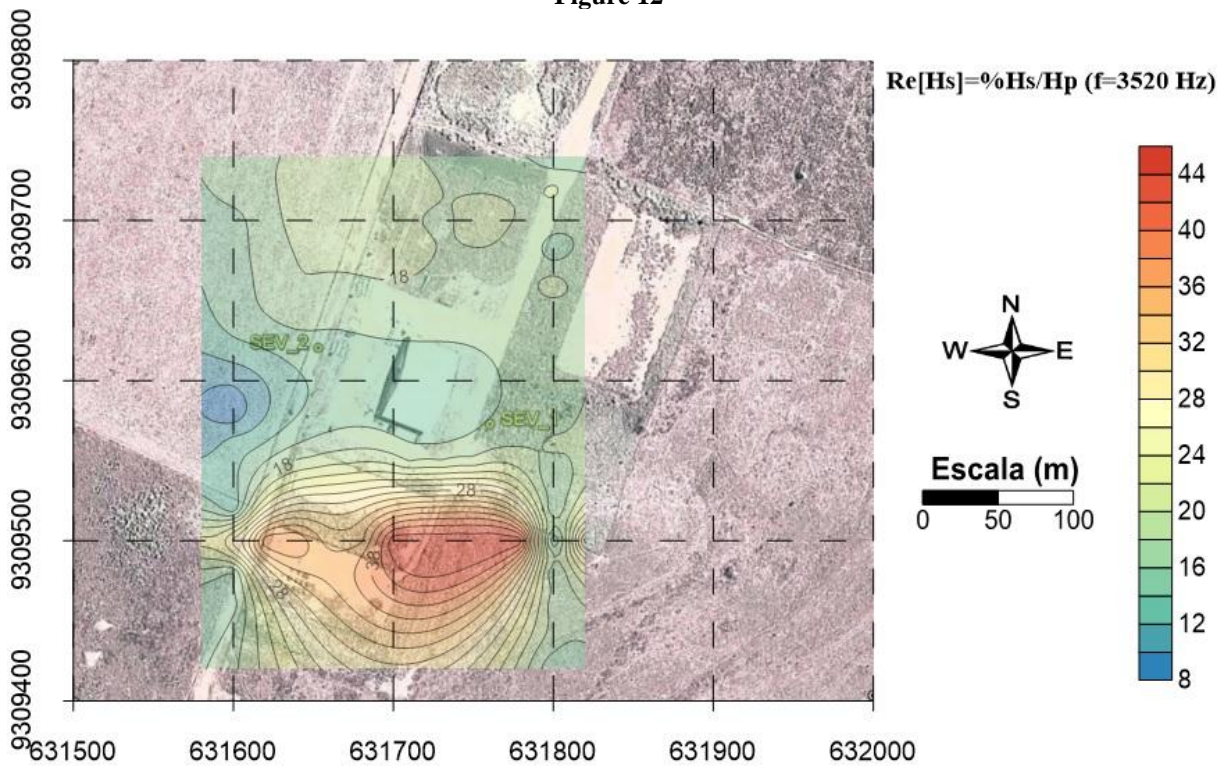


Figure 13

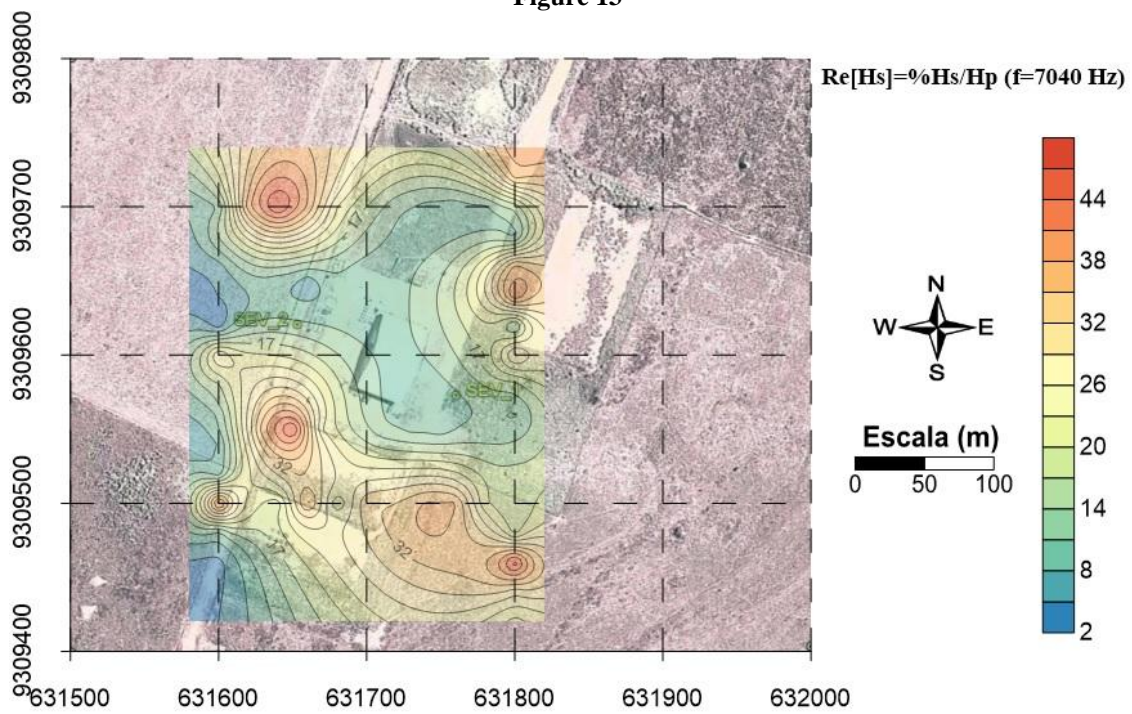
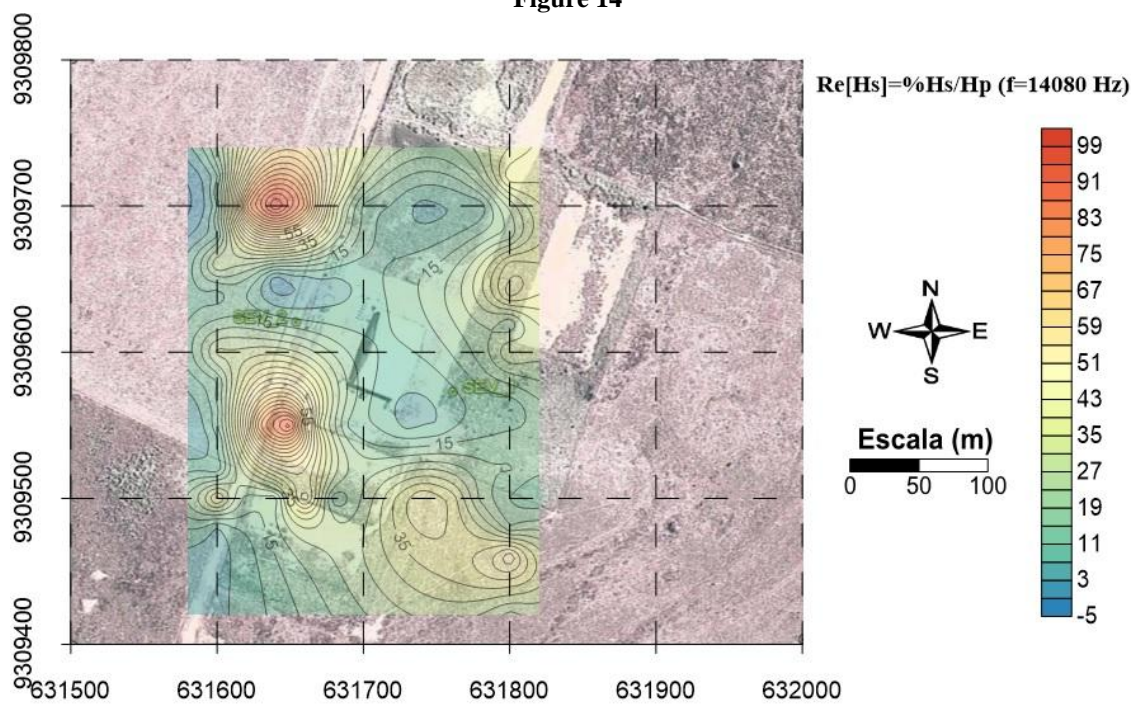
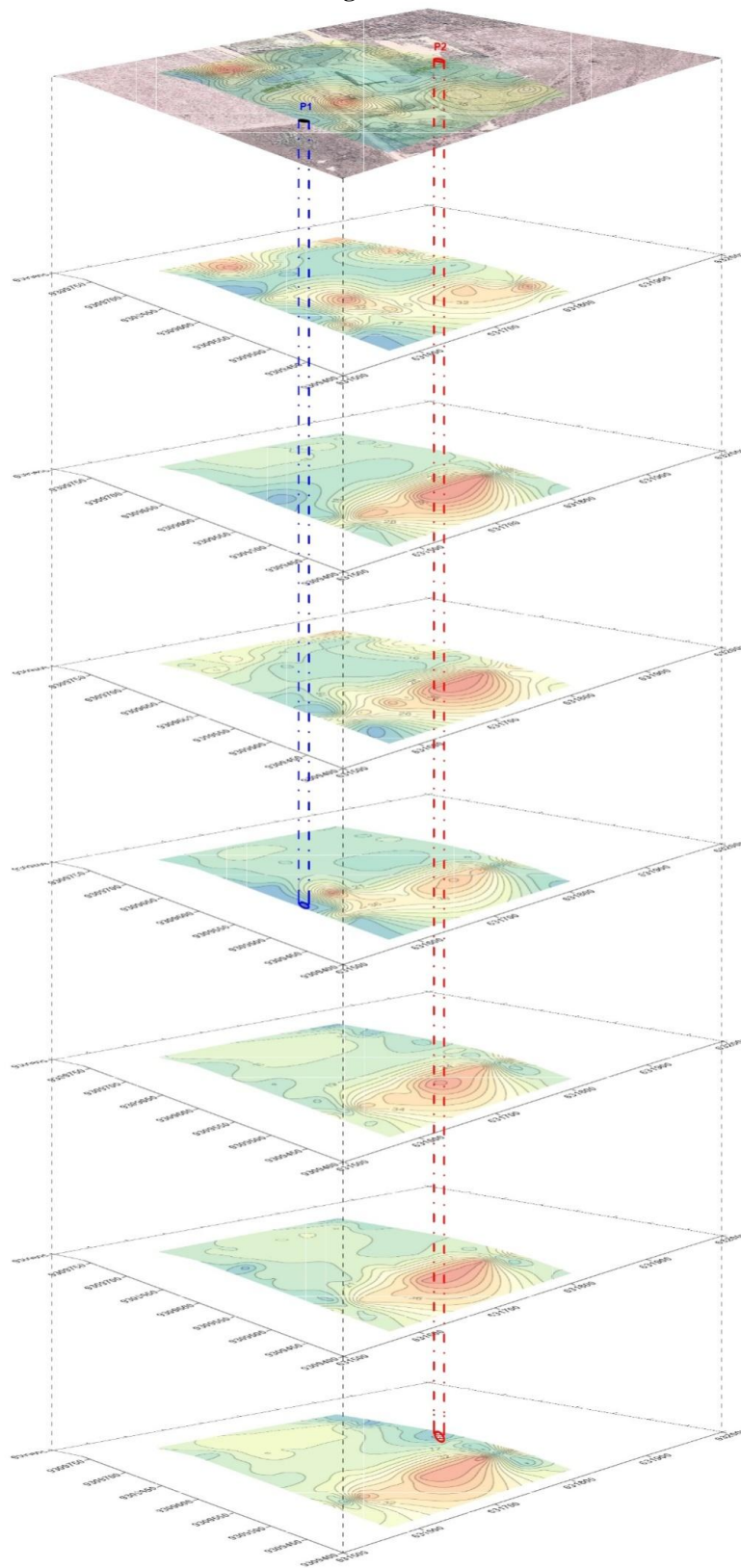


Figure 14



**Figure 15**



Herson Oliveira da Rocha. " Detection of aquifer zones by integration geophysical methods HLEM and VES in the Southeast region of Pará, Brazil."IOSR Journal of Applied Geology and Geophysics (IOSR-JAGG) 7.6 (2019): 01-14.